Final Report

ONR Contract #N00014-88-K-0094

"Fracton Dynamics"

June 12, 1990

Ralph V. Chamberlin
Department of Physics
Arizona State University
Tempe, AZ 85287

Introduction

We have made relaxation measurements of several systems over broad time ranges. We have developed[1] a general model for the relaxation of dispersive excitations on a percolation distribution of finite clusters which gives excellent agreement with the observed behavior. Using this model, simple relaxation measurements may be used as a unique tool for investigating the behavior of mesoscopic quantum correlations in complex systems.[2] Measurements of magnetic relaxation in spin glasses, ferromagnets and antiferromagnets, and stress relaxation in structural glasses provide new insight into the behavior of these materials.

Model

For percolation[3,4] we assume that two spins are correlated with probability p (presumably correlated means the electrons share the same multiparticle quantum-mechanical wave function, the spins need not be aligned). For p less than the critical concentration for bond percolation (p_c) there will be only finite domains of correlated spins, whereas for $p>p_c$ there is an infinite backbone in addition to finite domains. Percolation theory provides specific predictions for the probability that a given spin belongs to a domain of size s. For $p>p_c$ in 3 dimensions:[5] $sn_s=s^{1-\theta}\exp[-(C's)^{2/3}]$, where C' scales with $|p-p_c|^{1/\sigma}$, $\theta=-1/9$, and $\sigma=0.45$. If all domains are assumed to have identical initial susceptibility per spin (M_0), and if each domain is assumed to relax independently with a size-dependent relaxation rate (w_s), the net relaxation from all finite domains becomes $M(t)=M_0\sum_0^\infty(sn_s)e^{-w_st}$. For stochastic relaxation of quantized systems at temperature T, relaxation is due to activation between energy levels:[6] $w_s\propto e^{-\delta E/k_BT}$. All dispersive excitations on finite systems have an average energy-level spacing which is inversely proportional to the number of particles in the system:[7-9] $\delta E=\Delta/s$. This may be pictured (FIG. 1) from the fact that s discrete levels must fill a fixed magnon bandwidth (Δ depends only on the average interaction between particles, independent of cluster size). Using $x=C's$, the relaxation function becomes:

$$M(t)=M_{-}\int_0^{\infty}x^{10/9}\exp(-x^{2/3})\exp(-tw_{-}e^{-C_{-}/x})dx, \qquad \text{(Eq. 1)}$$

where $M_{-}=M_0C'^{\theta-2}|p-p_c|^{(\tau-\theta)/\sigma}$, $\tau=2.2$, $C_{-}=C'\Delta/k_BT$, and w_{-} is the relaxation rate of an "infinite" finite cluster (smaller clusters have larger energy-level spacing and hence relax more slowly). The preponderant relaxation is due to the dominant-sized domains [$\bar{x}=(19/6)^{3/2}$], but for $C_{-}>>1$ the spectrum is extremely broad.

For magnetic systems, the relaxation represented by Eq. 1 may be described as follows. A random probability of correlation between spins produces a percolation distribution of finite domains. At equilibrium in zero field, all domains have the same average internal energy (FIG. 1b). In an applied field (H), domains whose ground state magnetic moment is aligned with H have a lower internal energy (FIG. 1c). When H is removed, the internal energy of these domains must <u>increase</u> to the zero-field equilibrium. For domains whose net magnetic moment is antialigned with H (FIG. 1d), the internal energy must <u>decrease</u> to the zero-field equilibrium, resulting in the relaxation function:

$$M(t)=M_{+}\int_0^{\infty}x^{10/9}\exp(-x^{2/3})\exp(-tw_{+}e^{+C_{+}/x})dx. \qquad \text{(Eq. 2)}$$

Here the relaxation rate of an "infinite" finite cluster (w_{+}) is the slowest relaxation rate, since the energy-level spacing which drives its approach to equilibrium is the smallest.

Various mathematical approximation to Eqs. 1 and 2 reproduce several empirical functions previously used to characterize relaxation in random systems. Converting Eq. 1 or 2 to an integration over relaxation times, the distribution becomes: $n_\tau\sim\exp[28(\ln W)/9-W^{2/3}]/\tau$, where $W=\mp C_{\pm}/\ln(w_{\pm}\tau)$. To second-order in the exponent about its maximum, this is a log-normal distribution. Using a steepest descents approximation valid for $C_{-}w_{-}t>>1$, Eq. 1 becomes $M(t)\sim t^{-\alpha}$ with $\alpha\sim\bar{x}'[19-6(\bar{x}')^{2/3}]/(9C_{-})$, here $\bar{x}'$ is a time-averaged dominant-sized domain. A similar approximation for Eq. 2, valid when $C_{+}w_{+}t<<1$, reproduces the Kohlrausch-Williams-Watts stretched exponential: $M(t)\sim\exp(-t^{\beta})$ with $\beta=2/(5+3C_{+}/\bar{x}')$. Although various combinations of these empirical functions give good approximations to the observed behavior, data of sufficient quality and range invariably favor the percolation model.

per A197166

This model is quite general and may be applied to any random system with dispersive excitations (magnons, phonons, excitons, polaritons, etc). The percolation model may provide a physical basis for the universal relaxational behavior observed in many condensed matter systems.

Measurements

Magnetic relaxation measurements were made using a SQUID magnetometer coupled to a high-speed voltmeter. The measurements were made by applying a magnetic field (H=3.6 Oe) to a sample while at an elevated temperature. The sample was then field-cooled to the measurement temperature. After a specified wait-time ($t_w \sim 10^3$ sec), H was removed and the magnetization recorded as a function of time. Typically, the SQUID would flux-lock after 40-80 μsecs, and measurements were taken for 10^2-10^4 secs. The absolute magnetization was determined before, and after each relaxation by moving the sample between two counter-wound coils.

Random Magnetic Systems

We have measured random Au:Fe alloys with iron concentrations from 4% (spin glass) through 21% (random ferromagnet).[10] All exhibit similar relaxational behavior. The magnetization as a function of temperature of 11.9% Au:Fe shows a sharp maximum at T_m=39 K, characteristic of a concentrated spin glass. The magnetic relaxation for 3 temperatures above T_m is shown in FIG. 2. The accuracy of Eq. 1 is verified by the fact that no systematic deviations are observed throughout the time range of the fits (10^{-4}-10^1 sec) and that the curves extrapolate through the data at longer and shorter times (inset). The best fits to a simple power-law (inset, solid curves) give a good approximation to the data over 4-5 orders of magnitude in time, but significant deviations occur when the entire range of data is included.

Below T_m (FIG. 3) two regimes of relaxation are evident. A short time (<10 sec) power-law like regime, and a long-time (>10 sec) stretched-exponential like regime. Experimentally the data may be fit (solid curves) with identical distributions of aligned

and antialigned domains ($M_- = M_+ \equiv M_i$) with identical energy-level spacing ($C_- = C_+ \equiv C$):

$$M(t) = M_i \int_0^\infty x^{10/9} \exp(-x^{2/3}) [\exp(-t w_- e^{-C/x}) + \exp(-t w_+ e^{+C/x})]. \quad \text{(Eq. 3)}$$

Relaxation measurements of 19.8% Au:Fe (FIG. 4) reveal several complex features which may be explained in terms of the percolation model. Little relaxation occurs before $1/w_- = 30$ μsec. The locally steepest slope near $1/\varpi_- = 5$ msec is due to the relaxation of the dominant-sized aligned domains. Near $1/\varpi_+ = 80$ sec the magnetization again decreases more rapidly as the dominant-sized antialigned domains begin to relax. Negligible deviation between Eq. 3 (solid curve) and this complex behavior demonstrates the extreme accuracy of the percolation model.

The behavior of several physical parameters may be obtained from relaxation data using the percolation model. The intrinsic relaxation rates of "infinite" aligned (w_-) and antialigned (w_+) domains are obtained directly as fitting parameters. The relaxation rates of the dominant-sized aligned and antialigned domains (FIG. 5a) come from $\varpi_\pm = w_\pm \exp(\pm C/x)$. Other physical parameters such as the magnon bandwidth (Δ), initial thermoremanent magnetization per spin (M_0), and finite-domain correlation length (ξ) cannot be isolated from Eqs. 1-3 because x is a dummy variable of integration that connects them. If Δ is assumed to be constant, relative values may be obtained using $M_0 \propto M_i (\Delta/CT)^{\tau-2}$ and $\xi \propto (\Delta/CT)^{\sigma\nu}$, where $\tau = 2.2$, $\sigma = 0.45$, and $\nu = 0.88$ are percolation scaling exponents. The initial thermoremanent magnetization per spin (FIG. 5b) decreases linearly with increasing temperature up to the transition. The linear temperature dependence indicates a constant average energy-level spacing (δE) throughout this regime. Extrapolation to zero magnetization gives the temperature at which all magnons would be excited, providing an estimate for Δ; we find 43 ± 2 and 46 ± 2 K for 8.0% and 11.9% Au:Fe respectively. The correlation lengths (FIG. 5c) are a minimum at the transition (in contrast to a divergence if this were a percolation transition). Below the transition ξ also decreases linearly with increasing temperature, extrapolating to zero at 47 ± 4 and 49 ± 2 K for 8.0% and 11.9% Au:Fe respectively.

Dilute Au:Fe was the first random magnetic system to exhibit a sharp susceptibility cusp,[11] initiating interest in the possibility of a spin-glass transition. Indeed some thermodynamic transition may occur on the infinite backbone, but the accuracy of the percolation model indicates that mesoscopic quantum-correlated domains dominate the relaxational behavior. Above T_m, Eq. 1 implies that all domains are aligned with the magnetic field. In the vicinity of T_m, half the domains become antialigned. Below T_m, Eq. 3 indicates a well-defined energy-level distribution within each domain; randomness comes from size and orientational degeneracies between domains.

Structural Glasses

To verify the universality of the percolation model, we have reanalyzed some stress relaxation data[12] on the ionic conductor $AgI-AgPO_3$. Measurements were made by first warming the sample to near the glass temperature (T_g=88.5 ^oC). After an anneal time, a stress was applied and its relaxation recorded as a function of time (FIG. 6). Eq. 2 provides excellent agreement with the observed behavior (solid curves), indicating that a strain increases the level of phonon excitation, so that the average internal energy decreases to equilibrium. Using the percolation model, annealing may be characterized (inset) as an exponential softening of the localized phonon modes on a fixed distribution of percolation clusters.

Recent stress relaxation data (FIG. 7, in collaboration with R. Bohmer and C.A. Angell), are of sufficient quality and range to clearly demonstrate the superiority of the percolation model over empirical functions.

Review of Evidence in Support of the Percolation Model

Table I gives a statistical comparison of the χ^2 values from the percolation model versus the best previously used relaxation function with the same number of adjustable parameters. Every significant difference favors the percolation model.

SAMPLE	Au:Fe			AgI-Ag	
EMPIRICAL FUNCTION	8.0%	11.9%	19.8%	$-PO_3$	$-SO_4$
$t^{-\alpha}\exp[-(t/t_0)^{\beta}]$	$0.18\pm.09$	$-0.06\pm.11$	$1.02\pm.13$		
$\exp[-(t/t_0)^{\beta}]$				$0.02\pm.16$	$1.579\pm.012$

TABLE I. Average of $\ln(\chi^2/\chi_p^2)$ for various samples, where χ_p^2 is from the percolation model, and χ^2 the appropriate empirical function. Positive values indicate a better fit using the percolation model.

Additional evidence for the percolation model comes from the pleasingly simple behavior of the physical parameters. For Au:Fe at low temperatures, M_i and all empirical prefactors decrease linearly with increasing temperature, but drop more rapidly as the transition is approached. Considering only the fraction of spins which belong to finite clusters, the initial thermoremanent magnetization per spin (FIG. 5b) decreases linearly up to the transition. The correlation length (ξ) is roughly related to the empirical exponent β [for large ξ, a few very large finite domains dominate the behavior, and the relaxation is nearly exponential ($\beta \approx 1$)]. Near the spin-glass transition, β is found[13] to increase linearly with decreasing temperature, but saturates to a value of 0.3-0.4 below ~0.7 T_g. The linear behavior of ξ continues for all temperatures below T_g (FIG. 5c), furthermore, this saturation value arises naturally from the steepest-descents approximation to the percolation model.

Perhaps the greatest evidence for the percolation model, however, is the fact that this simple physical model provides a general basis for several empirical relaxation functions observed in condensed matter.

Antiferromagnet

Randomness for bond percolation need not come from intrinsic randomness in the sample, thermodynamic fluctuations will also produce random correlations in pure systems. To verify this, we measured magnetic relaxation in pure Neodymium.[14] Nd has two antiferromagnetic transitions; at 19.2 K the spins in alternate B

and C crystallographic planes antialign, and at 7.5 K the A planes antialign.

Magnetic relaxation of polycrystalline Nd is shown in FIG. 8. Least-squares fits to the data using Eq. 3 over the time range 10^{-4}-10^{1} sec (solid curves) reveal several features about this system. Eq. 3 provides excellent agreement over the fit range, indicating the presence of a percolation distribution of mesoscopic domains. These domains persist to at least 30 K, well above both transitions. Large deviations at long times may be attributed to other relaxation mechanisms (domain rotation and/or wall motion). Nevertheless, the percolation model provides excellent agreement with the observed behavior over 5-6 orders of magnitude in time; random correlation probabilities exist even in this elemental antiferromagnet.

Ferromagnet

Europium sulfide is one of the simplest magnetic systems available.[15] The magnetic moments are highly localized on the Eu sites in this non-metallic NaCl-like crystal. The anisotropy energy is very small (< 5 Oe) and EuS has been extensively studied as an ideal Heisenberg ferromagnet. The Curie temperature has been determined to be T_C=16.57±.02 K and the Weiss temperature (from high-temperature susceptibility measurements) is θ=18.7±1 K. We now briefly describe very recent (and preliminary) results on a spherical single crystal of this simple magnetic system.

The inverse magnetization of EuS as a function of temperature is shown in FIG. 9. Magnetic relaxation measurements at several temperatures in the vicinity of θ are shown in FIG. 10a. Above θ, Eq. 3 provides excellent agreement with the observed behavior (FIG. 10b) indicating that finite domains persist for temperatures well above T_C. A sharp increase in the remanence in the vicinity of θ may be due to mean-field behavior of these domains. Below θ (FIG. 11) the data can only be fit using unequal fractions of "aligned" and "antialigned" domains (Eq. 1 plus Eq. 2):

$$M(t)=\int_0^\infty x^{10/9}\exp(-x^{2/3})[M_-\exp(-tw_-e^{-C_-/x})+M_+\exp(-tw_+e^{+C_+/x})] \quad \text{Eq 4}$$

Although Eq. 4 has six adjustable parameters, the data show an obvious crossover near $1/w_+ = 4.95 \pm .09$ msec (marking the end of "antialigned" relaxation) so that the long-time data may be fit using Eq. 1, then the difference at short times fit using Eq. 2. The fact that Eq. 4 gives excellent agreement (solid curves) with the complex behavior indicates that fixed finite domains dominate the relaxation throughout the measurement range.

The temperature dependence of the aligned correlation length (FIG. 12) shows that the Curie transition is not a percolation transition, in fact ξ_- is extraordinarily small at T_C. Small ξ_- indicates small finite aligned domains, but since $p > p_c$ this means a high correlation probability ($p_- - p_c \propto \xi_-^{-1/\nu}$) and strongly aligned infinite backbone, as expected for a ferromagnetic transition.

Summary

A simple model for relaxation of dispersive excitations on a percolation distribution of finite clusters gives excellent agreement with measurements of stress relaxation in structural glasses and magnetic relaxation in spin glasses, ferromagnetic, and antiferromagnetic materials. The percolation model may provide a physical basis for the universal relaxational behavior observed in condensed matter. From the percolation model, simple relaxation measurements may be used to determine the size distribution, intrinsic response, energy-level spacing, and relaxational behavior of mesoscopic quantum correlations in complex systems.

REFERENCES

1. R.V. Chamberlin and D.N. Haines, submitted to Phys. Rev. Lett.
2. R.V. Chamberlin and D.N. Haines, to be published in proceedings of ONR Lake Arrowhead Contractors Meeting.
3. J.W. Essam, Rep. Prog. Phys. 43, 833 (1980).
4. D. Stauffer, A. Caniglio, and M. Adam, Adv. Polymer Science 44, 103 (1982); and Introduction to Percolation Theory, by D. Stauffer, Taylor & Francis, Philadelphia (1985).
5. T.C. Lubensky and A.J. McKane, J. Phys. A14, L157 (1981).
6. P. Hanggi and H. Thomas, Phys. Rep. 88, 207 (1982).
7. H. Frohlich, Physica 4, 406 (1937).
8. R. Kubo, J. Phys. Soc. Jpn. 17, 975 (1962).
9. R.F. Marzke, Catal. Rev. Sci. Eng. 19, 43 (1979).
10. B.V.B Sarkissian, J. Phys. F11, 2191 (1981).
11. V. Cannella, J.A. Mydosh, and J.I. Budnick, J. Appl. Phys. 42, 1689 (1971).
12. H.G.K. Sundar and C.A. Angell, XIV Intl. Congr. on Glass (1986), and C.A. Angell, H.G.K. Sundar, A.R. Kulkani, H. Senapati, and S.W. Martin, in Molecular Dynamics and Relaxation Phenomena in Glasses, Th. Dorfmuller and G. Williams eds., Springer-Verlag, Berlin, 1987, p.75.
13. R.V. Chamberlin, G. Mozurkewich, and R. Orbach, Phys. Rev. Lett. 52, 867 (1984).
14. S.K. Sinha in Handbook on the Physics and Chemistry of Rare Earths, vol. 1, K.A. Gschneidner and L. Eyring eds., North Holland, Amsterdam (1978).
15. P. Wachter, ibid, vol. 2.

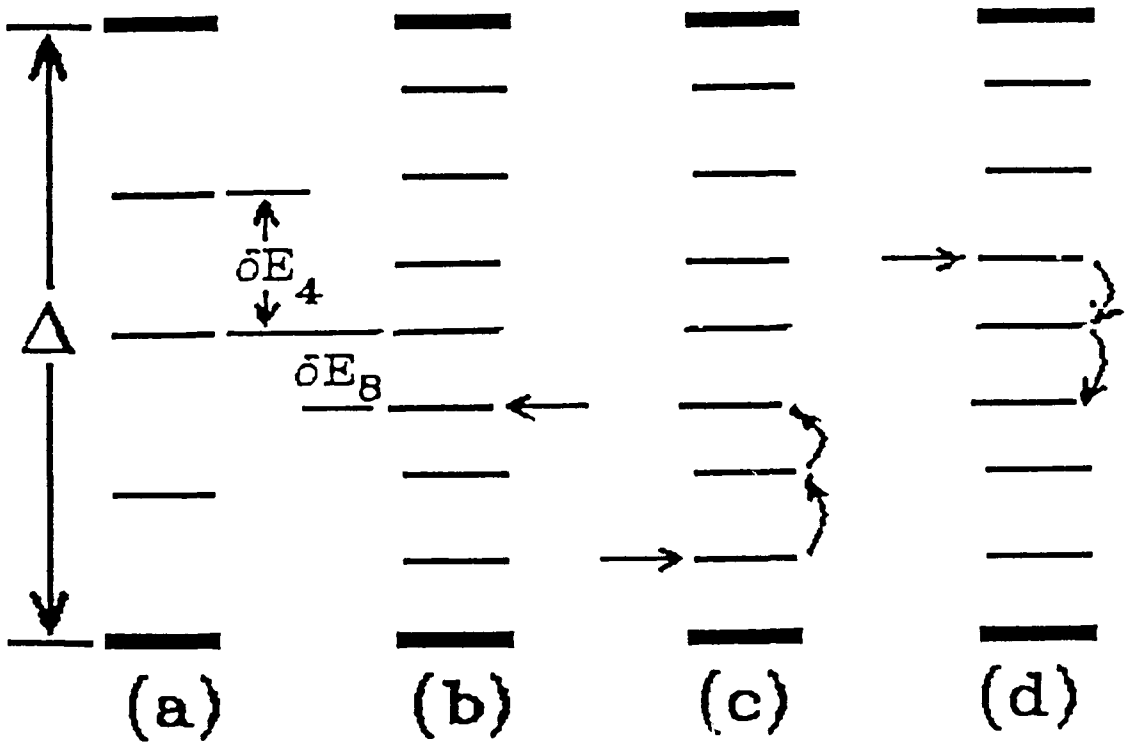

FIG. 1. Schematic representation of excitation levels in finite clusters. The bandwidth (Δ) is fixed by the average interaction between particles. (a)&(b) The average energy-level spacing (δE) varies inversely proportional to the number of particles in the cluster. (b) At equilibrium, all clusters have the same average internal energy. (c) For "aligned" clusters, whose energy was reduced by an external perturbation, the internal energy increases toward equilibrium. (d) The internal energy of "antialigned" clusters decreases when the external perturbation is removed.

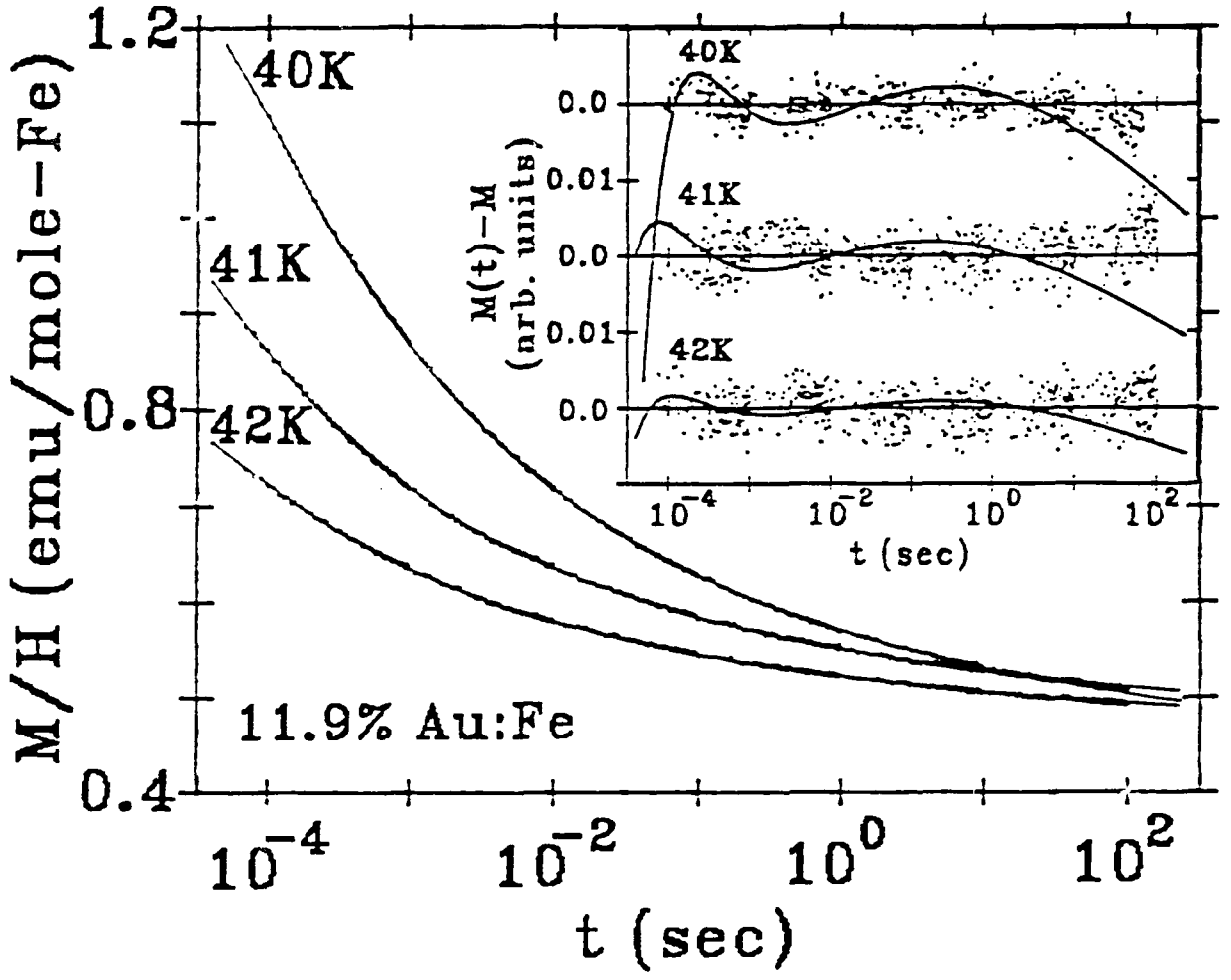

FIG. 2. Magnetic relaxation of 11.9% Au:Fe at 3 temperatures above the transition (T_m=39 K). The solid curves are the best fits using Eq. 1 over the range 10^{-4} to 10^{1} sec. No systematic deviation is observed from $<10^{-4}$ to 10^{2} sec. Inset shows the difference between Eq. 1 and the data. The best fits to a simple power-law (solid curves) are shown for comparison.

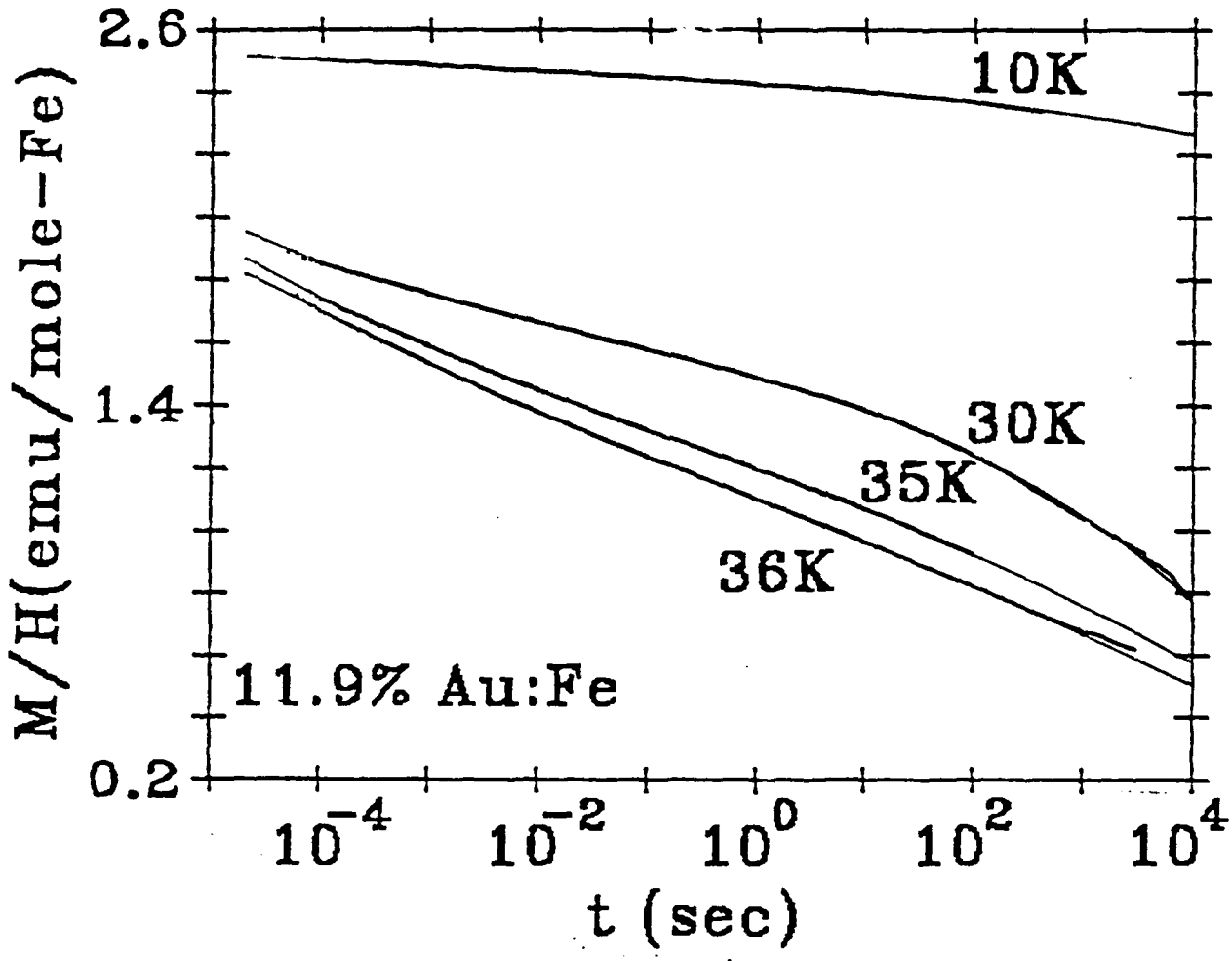

FIG. 3. Magnetic relaxation of 11.9% Au:Fe at 4 temperatures below T_m=39 K. The solid curves are the best fits using Eq. 3 over the range 10^{-4} to 10^{2} sec.

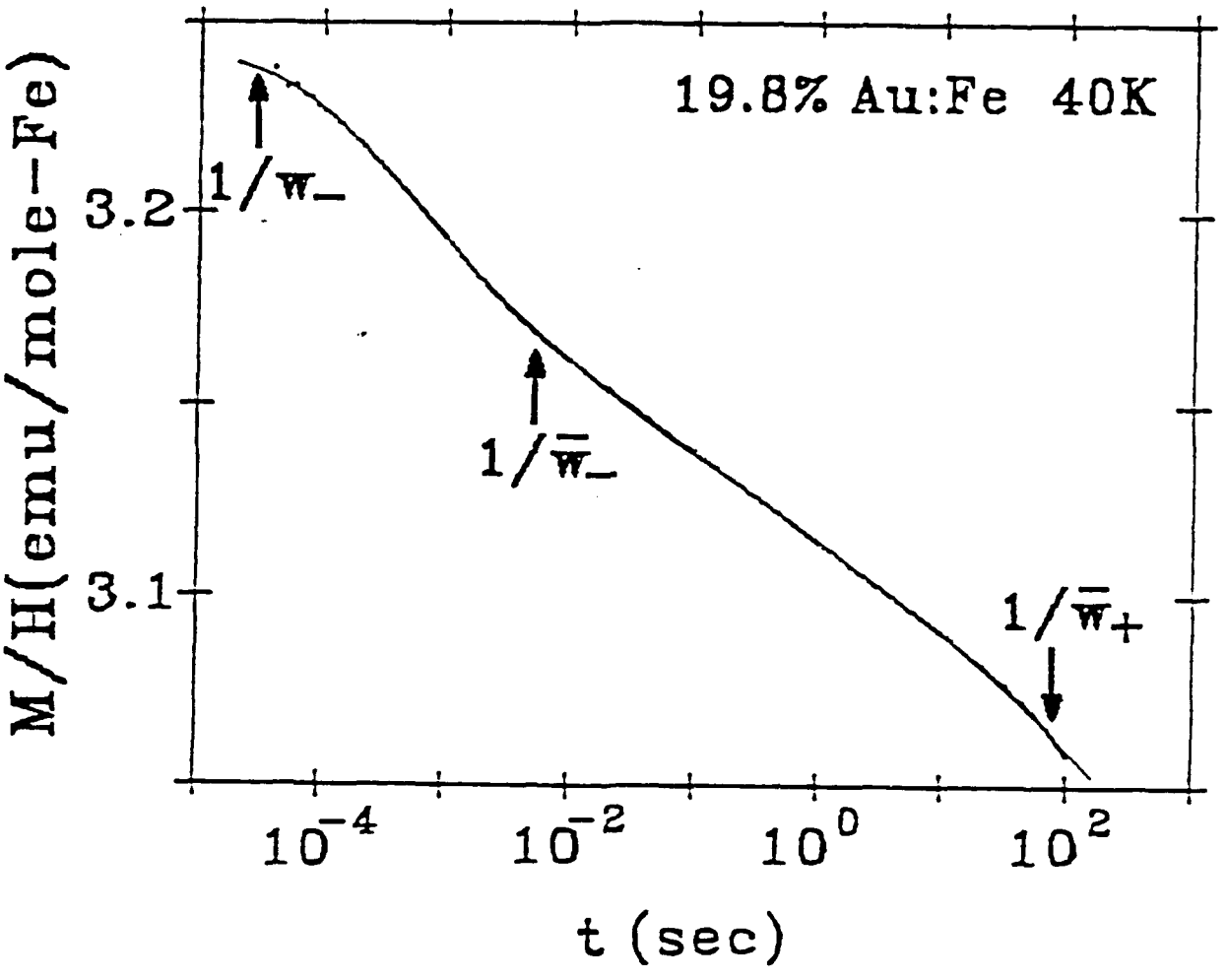

FIG. 4. Magnetic relaxation of 19.8% Au:Fe at 40 K. The solid curve is the best fit using Eq. 3. The complex behavior is due to the relaxation rates of the dominant-sized aligned ($1/\bar{w}_-$=5 msec) and antialigned ($1/\bar{w}_+$=80 sec) domains, and the broad distribution from $1/w_-$=30 μsec to $1/w_+$=10 ksec.

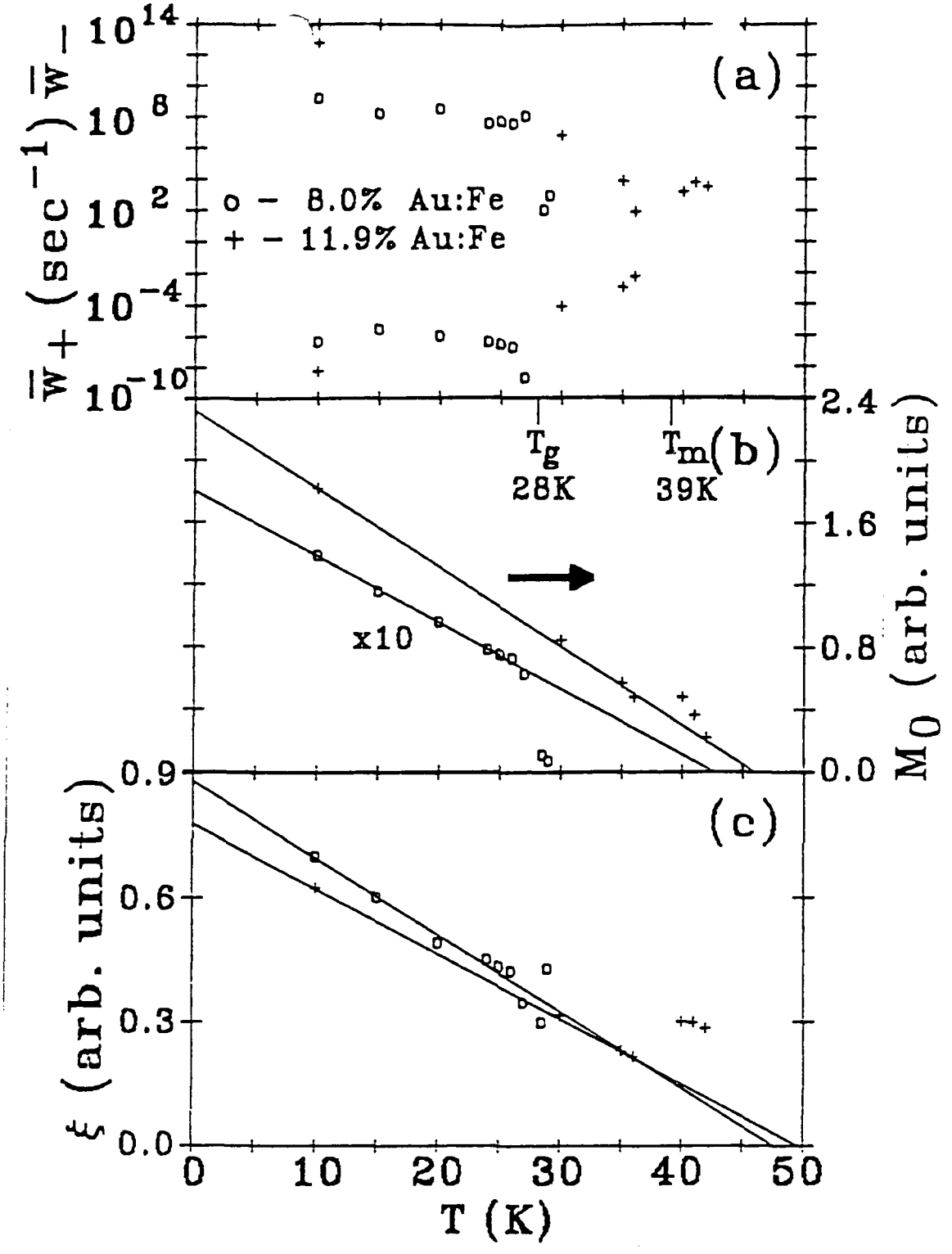

FIG. 5. (a) Temperature dependences of the dominant-sized aligned ($\bar{w}_-$, upper) and antialigned ($\bar{w}_+$, lower) relaxation rates for 8.0% (o) and 11.9% (+) Au:Fe. Solid curves are guides for the eye. Relative temperature dependences of (b) the initial thermoremanent magnetization per spin (M_0) and (c) the finite domain correlation length (ξ) for these samples. Solid lines are the best fits to the linear regimes below T_g=28 K and T_m=39 K.

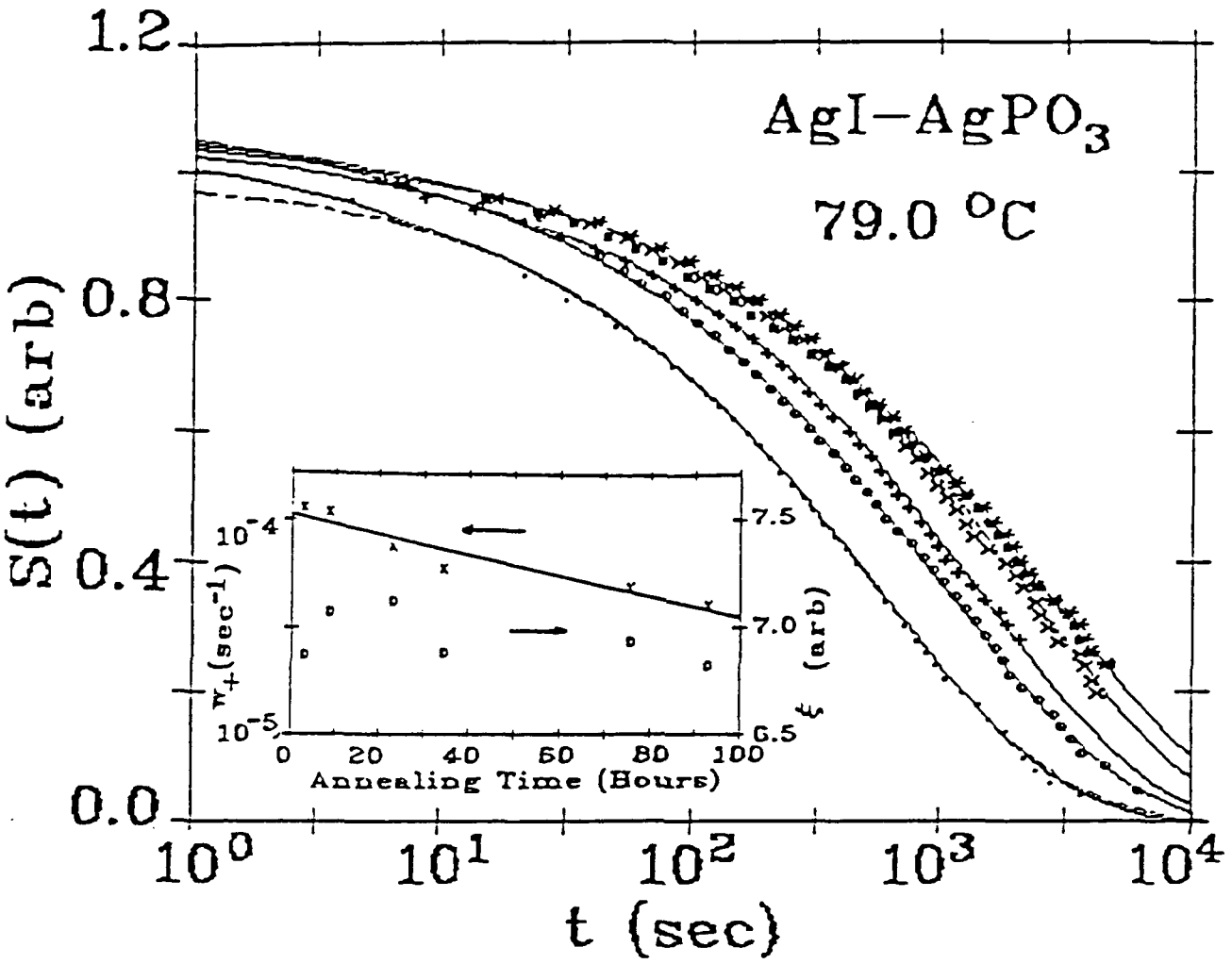

FIG. 6. Stress relaxation in AgI-$AgPO_3$ after annealing at 79.0 °C for ·-0, o-3, +-8.75, x-23.25, *-75.67, and ■-93 hours. Over the range of these data, Eq. 2 (solid curves) gives slightly better fits than the KWW stretched exponential (e.g. dashed curve). From the percolation model, annealing may be characterized (inset) as an exponential softening of the phonon relaxation rate (w_+) on finite molecular clusters with a constant correlation length (ξ).

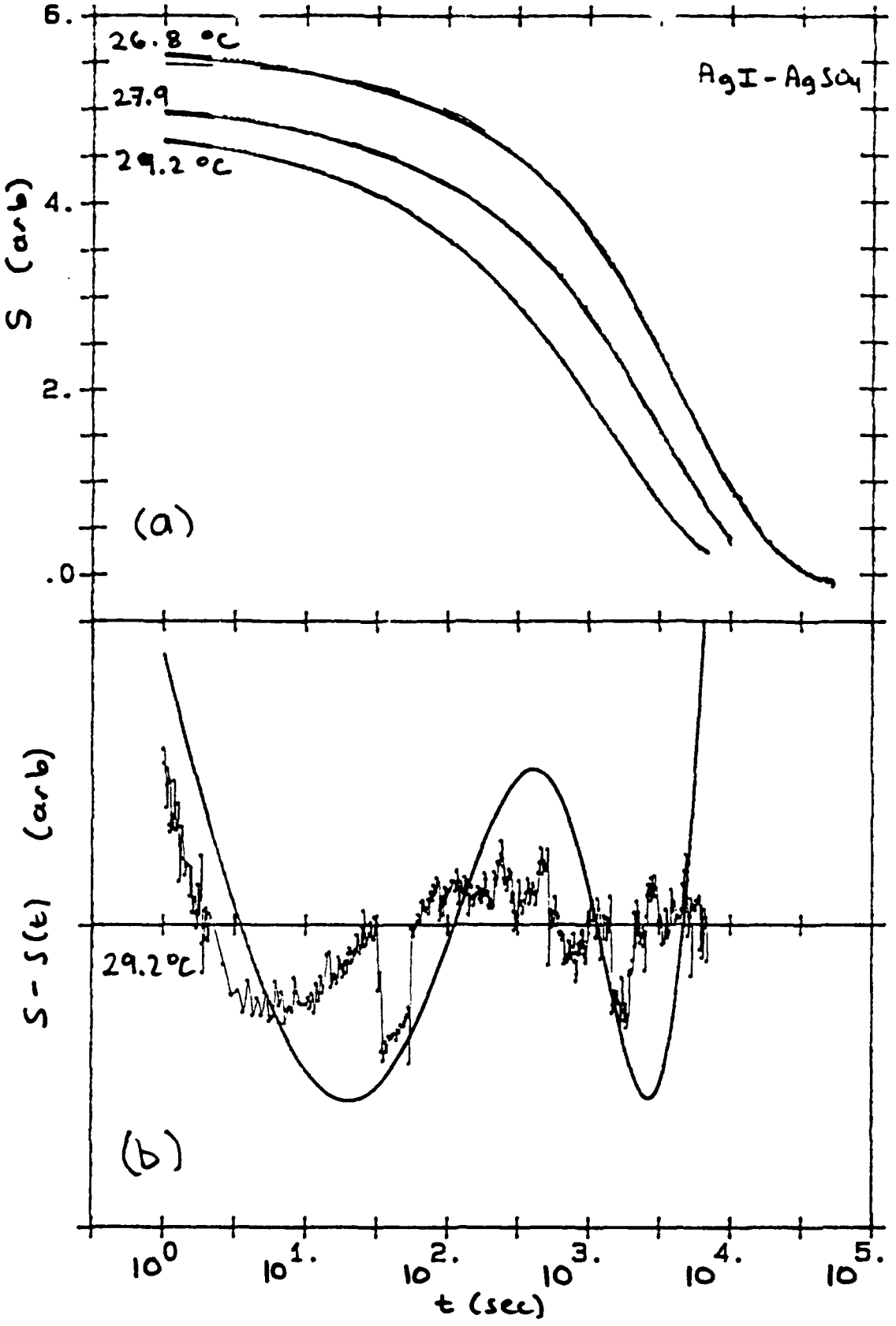

FIG. 7. (a) Stress relaxation in AgI-$AgSO_4$ at 3 temperatures below T_g=33 °C. The percolation model (Eq. 2, solid curves) gives much better fits than the KWW stretched exponential (dashed curves). (b) Difference between the data and Eq. 2 at 29.2 °C. The solid curve is the best fit using the empirical KWW function.

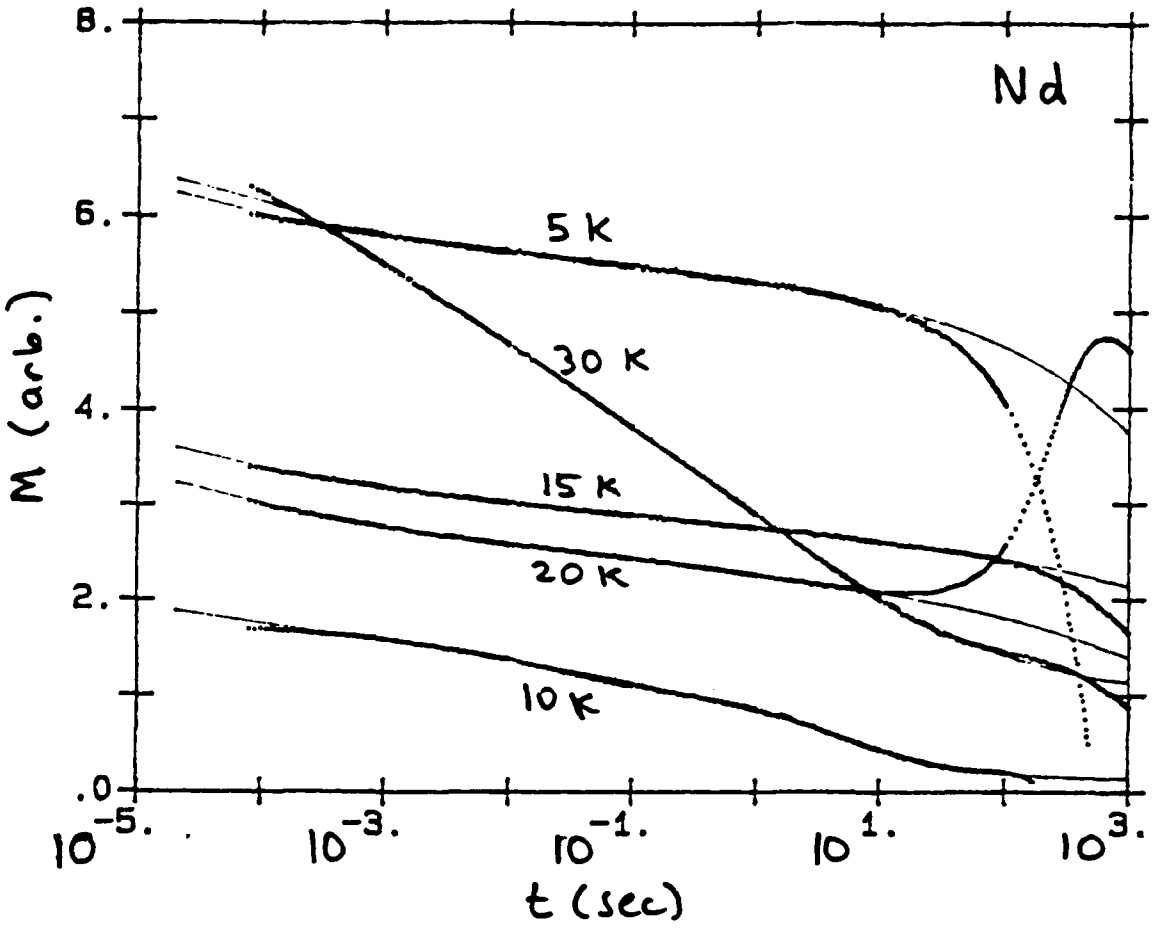

FIG. 8. Magnetic relaxation of Neodymium. The solid curves are the best fits using Eq. 3.

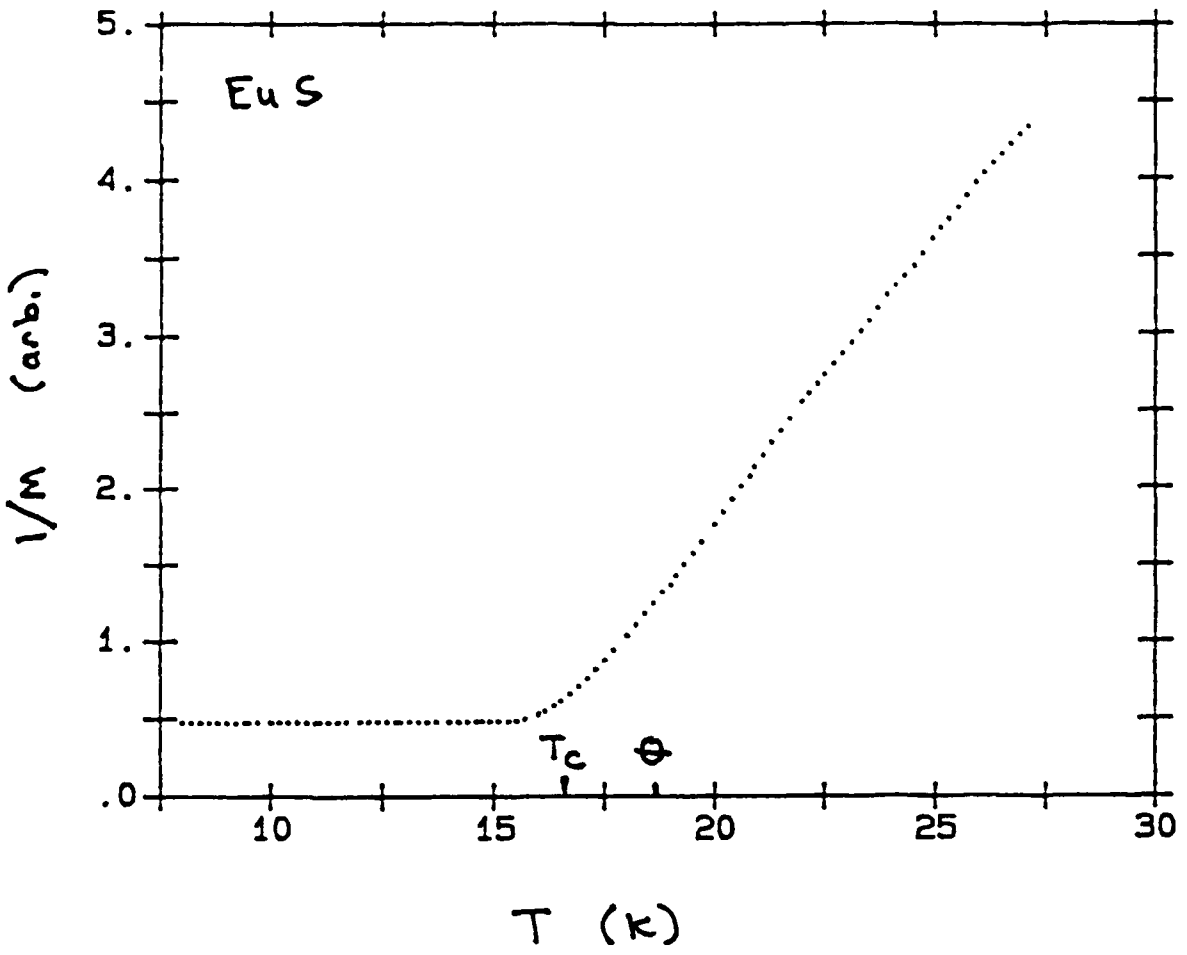

FIG. 9. Inverse magnetization versus temperature for a spherical single crystal of EuS. The Curie temperature is T_C=16.58±.02 K, and the Weiss temperature Θ=18.7±1 K.

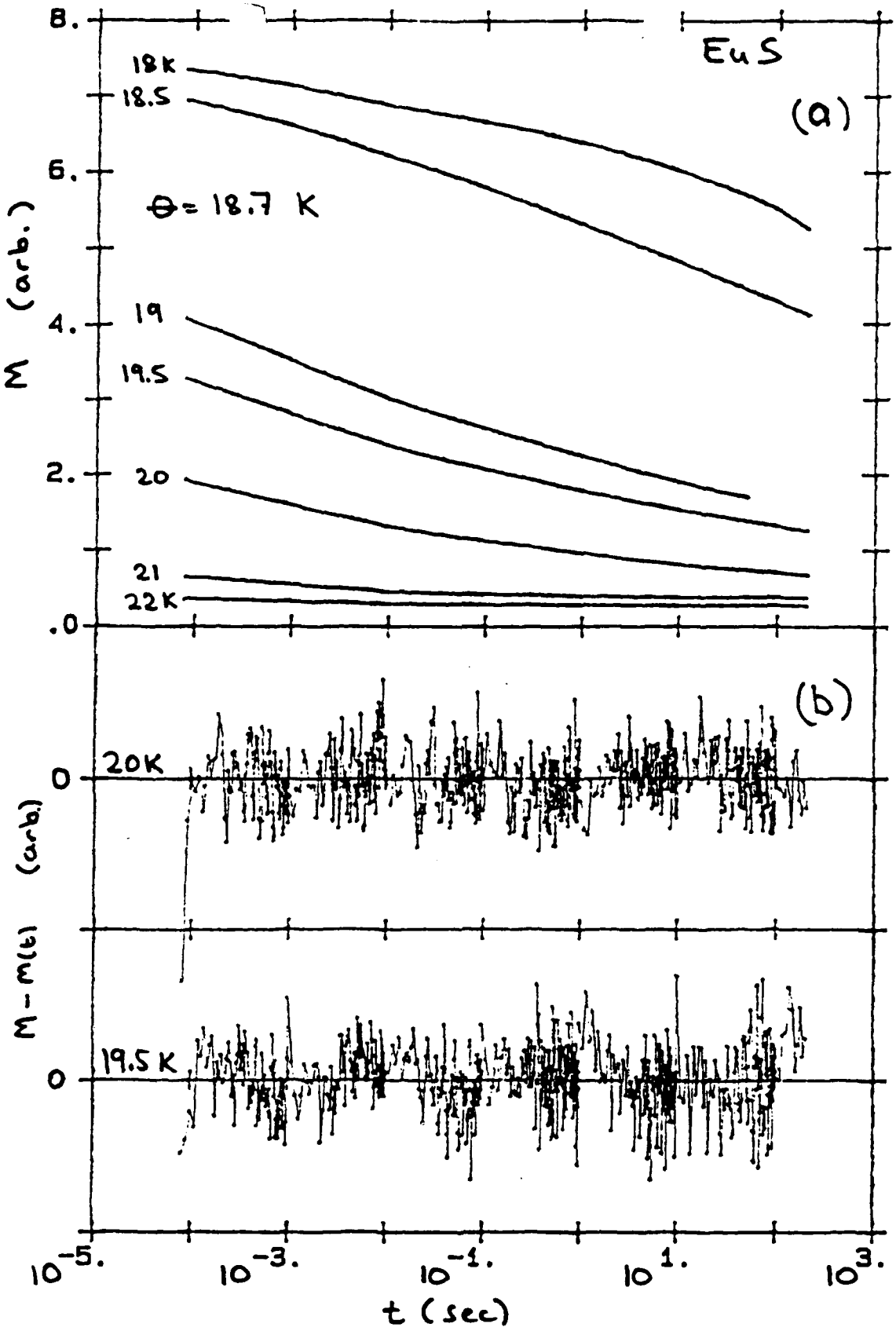

FIG. 10. (a) Magnetic relaxation of EuS at several temperatures in the vicinity of θ=18.7 K. (b) Deviation of the magnetic relaxation from Eq. 3 at two temperatures above θ.

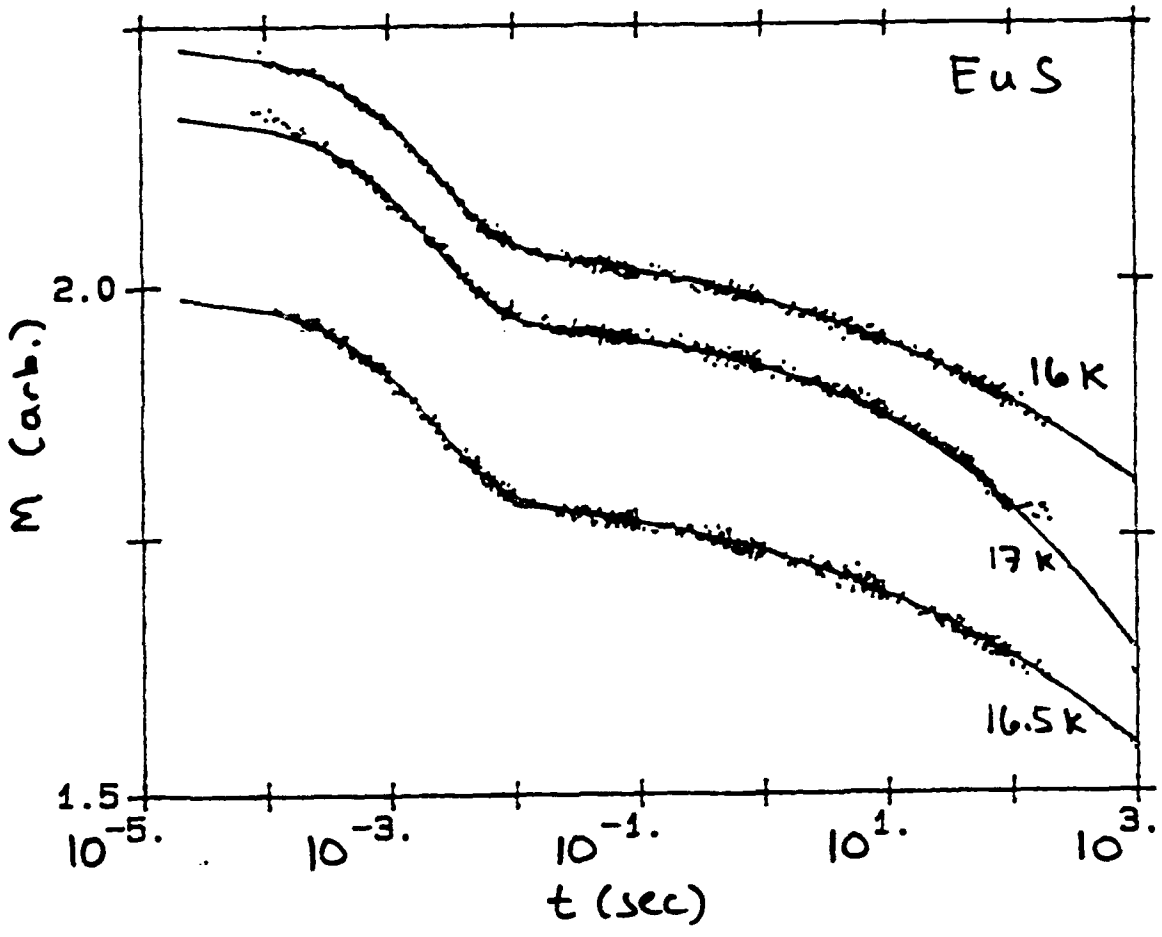

FIG. 11. Magnetic relaxation of EuS in the vicinity of T_C=16.58 K may be fit using unequal fractions of "aligned" and "antialigned" domains (Eq. 4, solid curves). The behavior near $1/w_+$=4.95±.09 msec signals the end of "antialigned" relaxation.

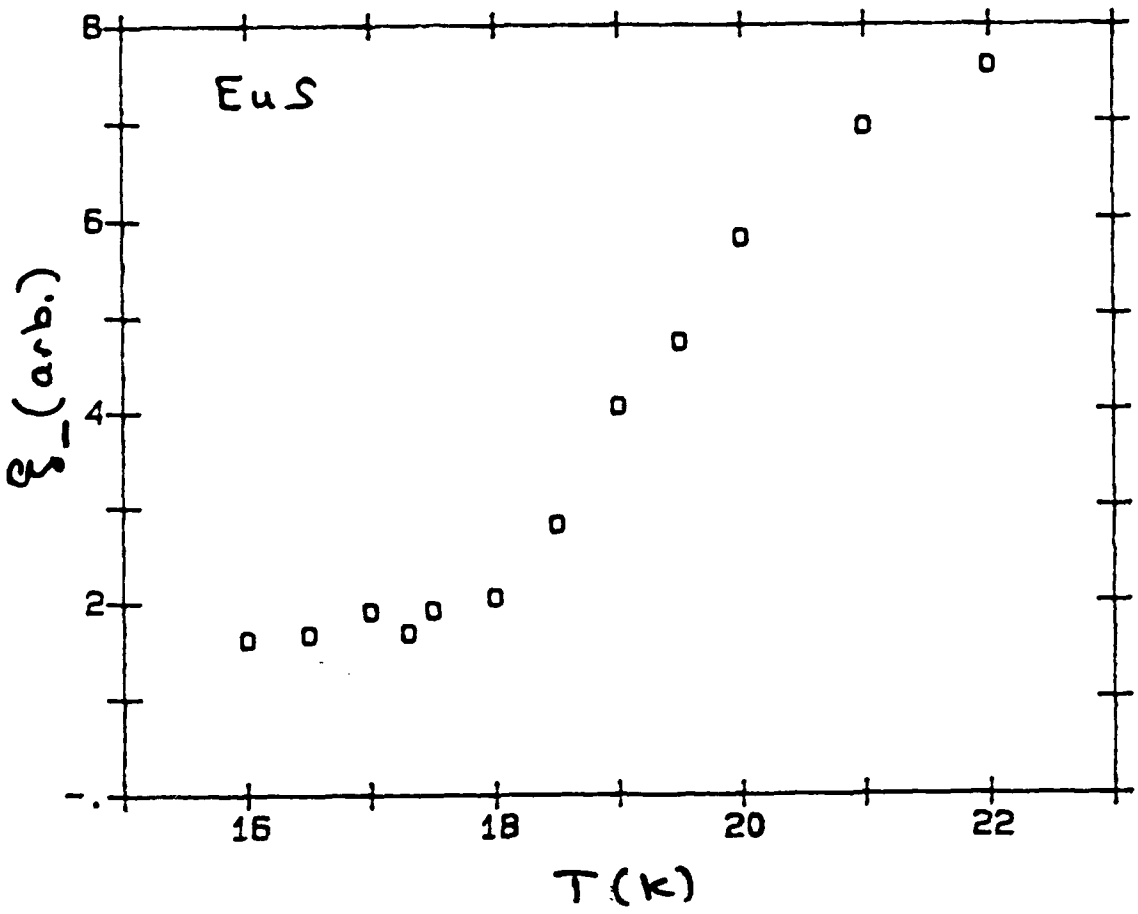

FIG. 12. Temperature dependence of the aligned correlation length. The relative value of ξ_- is extraordinarily small near T_C=16.58 K, indicating a highly correlated infinite backbone.